

Video Article

# Design and Implementation of a Bespoke Robotic Manipulator for Extra-corporeal Ultrasound

Shuangyi Wang<sup>1</sup>, James Housden<sup>1</sup>, Yohan Noh<sup>1</sup>, Anisha Singh<sup>2</sup>, Junghwan Back<sup>3</sup>, Lukas Lindenroth<sup>3</sup>, Hongbin Liu<sup>3</sup>, Joseph Hajnal<sup>1</sup>, Kaspar Althoefer<sup>4</sup>, Davinder Singh<sup>2</sup>, Kawal Rhode<sup>1</sup>

<sup>1</sup>School of Biomedical Engineering & Imaging Sciences, King's College London

<sup>2</sup>Xtronics Ltd

<sup>3</sup>Department of Informatics, King's College London

<sup>4</sup>Faculty of Science & Engineering, Queen Mary University of London

Correspondence to: Shuangyi Wang at [shuangyi.wang@kcl.ac.uk](mailto:shuangyi.wang@kcl.ac.uk)

URL: <https://www.jove.com/video/58811>

DOI: [doi:10.3791/58811](https://doi.org/10.3791/58811)

Keywords: Medical robot, robotic ultrasound, extra-corporeal ultrasound, robot design, mechanism design, linkages and manipulators, robot safety, 3D printing, rapid prototyping

Date Published: 12/23/2018

Citation: Wang, S., Housden, J., Noh, Y., Singh, A., Back, J., Lindenroth, L., Liu, H., Hajnal, J., Althoefer, K., Singh, D., Rhode, K. Design and Implementation of a Bespoke Robotic Manipulator for Extra-corporeal Ultrasound. *J. Vis. Exp.* (), e58811, doi:10.3791/58811 (2018).

## Abstract

With the potential for high precision, dexterity, and repeatability, a self-tracked robotic system can be employed to assist the acquisition of real-time ultrasound. However, limited numbers of robots designed for extra-corporeal ultrasound have been successfully translated into clinical use. In this study, we aim to build a bespoke robotic manipulator for extra-corporeal ultrasound examination, which is lightweight and has a small footprint. The robot is formed by five specially shaped links and custom-made joint mechanisms for probe manipulation, to cover the necessary range of motion with redundant degrees of freedom to ensure the patient's safety. The mechanical safety is emphasized with a clutch mechanism, to limit the force applied to patients. As a result of the design, the total weight of the manipulator is less than 2 kg and the length of the manipulator is about 25 cm. The design has been implemented, and simulation, phantom, and volunteer studies have been performed, to validate the range of motion, the ability to make fine adjustments, mechanical reliability, and the safe operation of the clutch. This paper details the design and implementation of the bespoke robotic ultrasound manipulator, with the design and assembly methods illustrated. Testing results to demonstrate the design features and clinical experience of using the system are presented. It is concluded that the current proposed robotic manipulator meets the requirements as a bespoke system for extra-corporeal ultrasound examination and has great potential to be translated into clinical use.

## Video Link

The video component of this article can be found at <https://www.jove.com/video/58811/>

## Introduction

An extra-corporeal robotic ultrasound (US) system refers to the configuration in which a robotic system is utilized to hold and manipulate a US probe for external examinations, including its use in cardiac, vascular, obstetric, and general abdominal imaging<sup>1</sup>. The use of such a robotic system is motivated by the challenges of manually holding and manipulating a US probe, for instance, the challenge of finding standard US views required by clinical imaging protocols and the risk of repetitive strain injury<sup>2,3,4</sup>, and also by the needs of US screening programs, for instance, the requirement for experienced sonographers to be on-site<sup>5,6</sup>. With emphases on different functionalities and target anatomies, several robotic US systems, as reviewed in earlier works<sup>1,7,8</sup>, have been introduced since the 1990s, to improve different aspects of US examination (e.g., long-distance teleoperation<sup>9,10,11,12</sup>, as well as robot-operator interaction and automatic control)<sup>13,14</sup>. In addition to the robotic US systems used for diagnostic purposes, robotic high-intensity focused ultrasound (HIFU) systems for treatment purposes have been widely investigated as summarized by Priester *et al.*<sup>1</sup>, with some recent works<sup>15,16</sup> reporting the latest progress.

Although several robotic US systems have been developed with relatively reliable technologies for control and clinical operation, only a few of them have been successfully translated into clinical use, such as a commercially available tele-ultrasound system<sup>17</sup>. One possible reason is the low level of acceptance for large-size industrial-looking robots working in a clinical environment, from the point of view of both patients and sonographers. Additionally, for safety management, the majority of the existing US robots rely on force sensors to monitor and control the applied pressure to the US probe, while more fundamental mechanical safety mechanisms to limit the force passively are usually not available. This may also cause concerns when translating into clinical use as the safety of robot operation would be purely dependent on electrical systems and software logic.

With the recent advancements of 3D printing techniques, specially shaped plastic links with custom-made joint mechanisms could provide a new opportunity for developing bespoke medical robots. Carefully designed lightweight components with a compact appearance could improve clinical acceptance. Specifically for US examination, a bespoke medical robot aimed at being translated into clinical use should be compact, with

enough degrees of freedom (DOFs) and range of motion to cover the region of interest of a scan; for example, the abdominal surface, including both the top and sides of the belly. Additionally, the robot should also incorporate the ability to perform fine adjustments of the US probe in a local area, when trying to optimize a US view. This usually includes tilting movements of the probe within a certain range, as suggested by Essomba *et al.*<sup>18</sup> and Bassit<sup>19</sup>. To further address the safety concerns, it is expected that the system should have passive mechanical safety features which are independent of electrical systems and software logic.

In this paper, we present the detailed design and assembly method of a 5-DOF dexterous robotic manipulator, which is used as the key component of an extra-corporeal robotic US system. The manipulator consists of several lightweight 3D-printable links, custom-made joint mechanisms, and a built-in safety clutch. The specific arrangement of the DOFs provides full flexibility for probe adjustments, allowing easy and safe operations in a small area without colliding with the patient. The proposed multi-DOF manipulator aims to work as the main component that is in contact with patients and it can be simply attached to any conventional 3-DOF global positioning mechanism to form a complete US robot with fully active DOFs to perform a US scan.

## Protocol

### 1. Preparation of Each Link, End-effector, and Additional Components

1. Print all the links ( $L_0$ ,  $L_1$ ,  $L_2$ ,  $L_3$ , and  $L_4$ ) and the end-effector as shown in **Figure 1**, with acrylonitrile butadiene styrene (ABS) plastic, polylactic acid (PLA) plastic, or nylon, using a 3D-printing service. Use the .STL files provided in the **Supplementary Materials** when printing. NOTE: Changes in shape and scale of each part can be made based on the provided files. The inner profile of the end-effector can be changed to fit different US probes.
2. Print all the required additional components as shown in **Figure 2** in nylon, using a 3D-printing service. Refer to the **Table of Materials** for the required number of each component. Use the .STL files provided in the **Supplementary Materials** when printing.
3. Polish all the printed plastic parts with polishing tools if necessary. Remove any supporting materials left from 3D printing, if necessary. NOTE: Some structures in the provided end-effector design are for a force sensor, which is not a part of the protocol reported here and will not be used for the assembly. The force sensor design concept has been reported in previous work<sup>20</sup>; thus, it is not covered in this paper.

### 2. Assembly of Joint 1

NOTE: The assembly of joint 1 ( $J_1$ ) is based on **Figure 3**.

1. Place the four small, geared stepper motors (with 20-teeth spur gears attached) into the mounting cavities of  $L_0$  and mount them with screws.
2. Place the two 37 mm OD bearings into the bearing housings of  $L_0$  and secure the 120-teeth spur gear (Type A) onto the hexagon key of  $L_1$ .
3. Insert the shaft on  $L_1$  into the shaft hole on  $L_0$  with the four small driving spur gears and the large, driven spur gear engaged, and assemble the shaft collar to secure and retain the shaft.

### 3. Assembly of Joint 2

NOTE: The assembly of joint 2 ( $J_2$ ) is based on **Figure 4**.

1. Place the four small, geared stepper motors (with 20-teeth spur gears attached) into the mounting cavities of  $L_1$  and mount them with screws.
2. Attach the two 120-teeth spur gears (Type B) to the two 37 mm OD bearings and position them into the gear cavities of  $L_1$ , with the 120-teeth spur gear (Type B) engaged with the 20-teeth spur gears mounted on the motors. Unscrew and re-screw the motor if necessary to allow the easy positioning of the two 120-teeth type-B spur gear.
3. Align  $L_1$  and  $L_2$  and insert the bearing and the ball-spring pairs into the clutch holes in  $L_2$ . With the two round clutch covers aligning and pushing the spring into the clutch mechanism for preloading, insert an M6 bolt into the bores of  $L_1$  and  $L_2$ .
4. Rotate the assembly to the other side and repeat steps in 3.3 for this side. Secure the assembly by attaching a nut to the M6 bolt.

### 4. Assembly of Joint 3

NOTE: The assembly of joint 3 ( $J_3$ ) is based on **Figure 5**.

1. Place the two small, geared stepper motors (with 20-teeth spur gears attached) into the mounting cavities of  $L_2$  and mount them with screws.
2. Place the 37 mm OD bearing into the bearing housing of the 120-teeth spur gear (Type C) and place the 32 mm OD bearing into the bearing housing of  $L_3$ .
3. Secure the large spur gear into the hexagon keyhole of  $L_3$  (additional screws can be used if necessary) and insert the shaft on  $L_2$  into the bores on the large spur gear and  $L_3$ , with the small and the large spur gears engaged.

### 5. Assembly of the Driving Mechanism of Joint 4

NOTE: The assembly of joint 4 ( $J_4$ ) is based on **Figure 6**.

1. Place the two small, geared stepper motors into the mounting cavities of  $L_3$  and mount them with screws. Place the 8 mm OD bearings into the bearing housings of  $L_4$ .
2. Mount the 20-teeth long spur gear onto the two small stepper motors.

## 6. Assembly of the Driven Mechanism of Joint 4 and Joint 5

NOTE: The assembly of joint 4 ( $J_4$ ) is based on **Figure 6** and joint 5 ( $J_5$ ) is based on **Figure 7**.

1. Position the driven 144 teeth bevel gear onto the extrusion of  $L_4$ .
2. Place the two small, geared stepper motors (with 18-teeth bevel gears attached) into the mounting cavities of  $L_4$  and mount them with screws. Finally, insert the M5 shaft into the shaft hole of  $L_3$  and  $L_4$  after the two links are aligned. Ensure the built in driven gear structures on  $L_4$  matches with the 20 teeth long spur gear.
3. Insert the end-effector into the keyway of the large bevel gear and vertically position the end-effector with the end-effector collar screwed onto it.

### Representative Results

Following the protocol, the resulting system is a robotic manipulator with five specially shaped links ( $L_0$  to  $L_4$ ) and five revolute joints ( $J_1$  to  $J_5$ ) for moving, holding, and locally tilting a US probe (**Figure 8**). The top rotation joint ( $J_1$ ), with gear mechanisms actuated by four motors, can rotate the following structures  $360^\circ$ , to allow the US probe to point toward different sides of the scanning area, such as the top, bottom, and sides of the abdomen. The main tilting joint ( $J_2$ ), with gear mechanisms actuated by four motors, is used to tilt down the probe to align it with the surface of the scanning area. As this joint is also crucial to the force management, a mechanical clutch with balls, springs, and detent holes was incorporated. The last three orthogonal revolute joints ( $J_3$ ,  $J_4$ , and  $J_5$ ), with gear mechanisms actuated by two motors each, are used to control the tilting and axial rotation of the probe, allowing fine adjustments of the probe in a local area. The last revolute joint,  $J_5$ , also allows the mounting of a US probe in a specially shaped end-effector. The total weight and length of the proposed robotic manipulator, which is the only structure usually on top of the patient's body, are less than 2 kg and 25 cm. The resulting design is such that a large range of probe positions can be reached with only small movements of the remaining global positioning mechanism when using the proposed robotic US manipulator. Considering just the proposed manipulator on its own, the probe can be rotated axially to any angle, tilted to follow a surface angled between  $0^\circ$  and  $110^\circ$  to the horizontal in any direction, and positioned within a circle with a diameter of 360 mm. Additionally, the revolute joints  $J_3$  and  $J_4$  provide a tilting angle, in two directions, in the ranges of  $-180^\circ$  to  $180^\circ$  and  $-30^\circ$  to  $45^\circ$ , which is used for local fine adjustments of the US probe. The ranges of movements and tilting angles meet the required ranges for obtaining an ideal acoustic window for US examinations as suggested by Essomba *et al.*<sup>18</sup> and Bassit<sup>19</sup>. The technical details of the proposed robotic manipulator are summarized in **Table of Materials** (Denavit-Hartenberg parameters and joint specifications), based on the coordinate definitions shown in **Figure 8**. The estimated cost of the system is 500 GBP, based on the current manufacturing method, components, and materials.

As an example used in this research, we employed a global positioning system which has a revolute joint ( $R_1$ ) with a chain mechanism for rotating the complete arm and a two-bar arm-based set of parallel link mechanisms ( $R_2$  and  $R_3$ ) with worm-gear drives (**Figure 9**). This 3-DOF mechanism will work with the proposed 5-DOF manipulator to form a complete robotic US system. Based on the proposed robotic manipulator and the example global positioning option used for this research, **Figure 10** shows a simulation example of the robot in positions around an abdominal phantom, demonstrating that it is able to reach around both sides of the abdomen and a range of positions on top. The design of the redundant joints in the system, particularly the configurations of  $J_1$  and  $J_2$ , allows tilting the probe to large angles with most of the mechanical structures still staying away from the patient's body, as can be observed in **Figure 10**. Consequently, with the last three joints ( $J_3$ ,  $J_4$ , and  $J_5$ ) specified to rotate within limited ranges for fine tilting adjustments, collision is avoided between the moving parts of the robot and the patient's body.

With the electronics and the conventional stepper motor control system developed, experiments have been performed to test the output force and validate the expected range of motion. The current control unit is a box with microcontrollers, stepper motor drivers, power supply and regulators, and other supporting electronic components included. The overall size of the control box is 40 cm long, 23 cm wide, and 12 cm deep. Based on the repeated testing of the system, the maximum force which the robotic manipulator can currently exert is set to 27 N before the mechanical safety clutch is triggered, specifying the output force range of the proposed system to be 0 - 27 N. With the configuration of the mechanical clutch, it was verified by repeated testing that in the default position, when the clutch is engaged, the balls are partially in the detent holes of  $L_1$ . Therefore, the movements of the driven, large spur gears actuate  $L_2$ . However, when excessive force is exerted at the end-effector, the clutch is disengaged, with the balls moving out of the detent holes of  $L_1$ .

The range of motion of each joint reported in **Table of Materials** was also repeatedly tested and validated. The reliable working of the robotic manipulator over a long period of time has been extensively tested on a fetal phantom and continuously verified with abdominal scans of internal healthy volunteers (**Figure 11**). The study was approved by the local ethics committee. So far, 20 volunteer scans for general abdominal ultrasound examinations using the robotic manipulator have been successfully performed with the basic software control of the robot, mainly to evaluate the reliability and feasibility of the mechanical design. It was concluded from the phantom and volunteer studies that the current design of the robotic manipulator can reach the required movement range at the required force, and provides enough fine adjustment to obtain images similar to the hand-held operation of the US probe for abdominal imaging. For all these scans, no safety concerns or uncomfortable feelings were reported by the volunteers. The selection of motors, mechanical ratios of mechanisms, and power levels have been verified such that they ensure the reliable movement of the probe on the patient's body, while at the same time resulting in slippage if excess forces are generated. Further details of this on-going volunteer study and clinical evidence for the use of the robot will be presented separately.

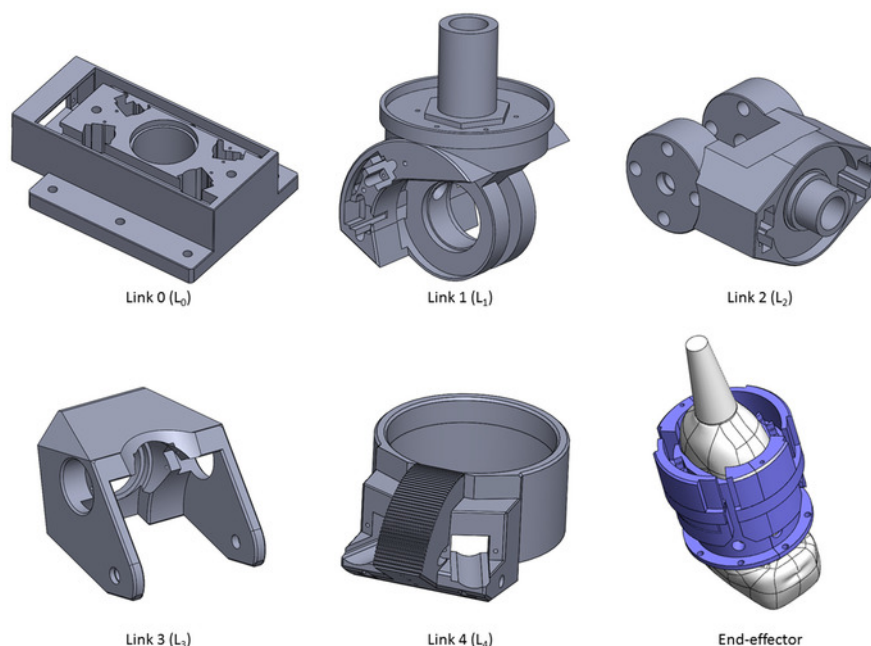


**Figure 1: Computer-aided design (CAD) drawing of all the links ( $L_0$ ,  $L_1$ ,  $L_2$ ,  $L_3$ , and  $L_4$ ) and the end-effector.** The shape of each link is shown for reference when 3D printing using the provided .STL files. The end-effector is illustrated with a US probe included in the assembly. [Please click here to view a larger version of this figure.](#)

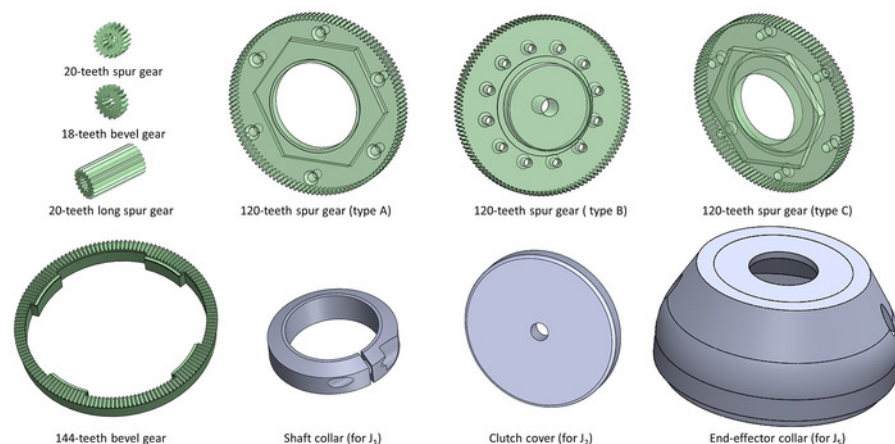


**Figure 2: CAD drawing of the required additional components.** The shape of each component is shown for reference when 3D printing using the provided .STL files. The components include spur and bevel gears in different sizes, a shaft collar, a clutch cover, and an end-effector collar. [Please click here to view a larger version of this figure.](#)

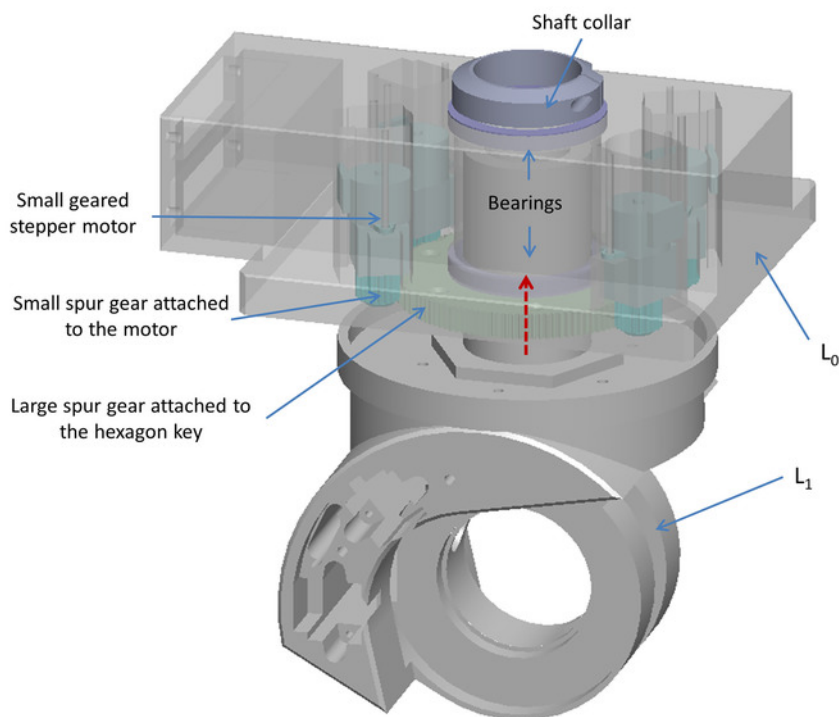


**Figure 3: Assembly instruction for J<sub>1</sub>.** The required links, motors, gears, and bearings are shown, with some structures changed to transparent to illustrate the assembly. [Please click here to view a larger version of this figure.](#)

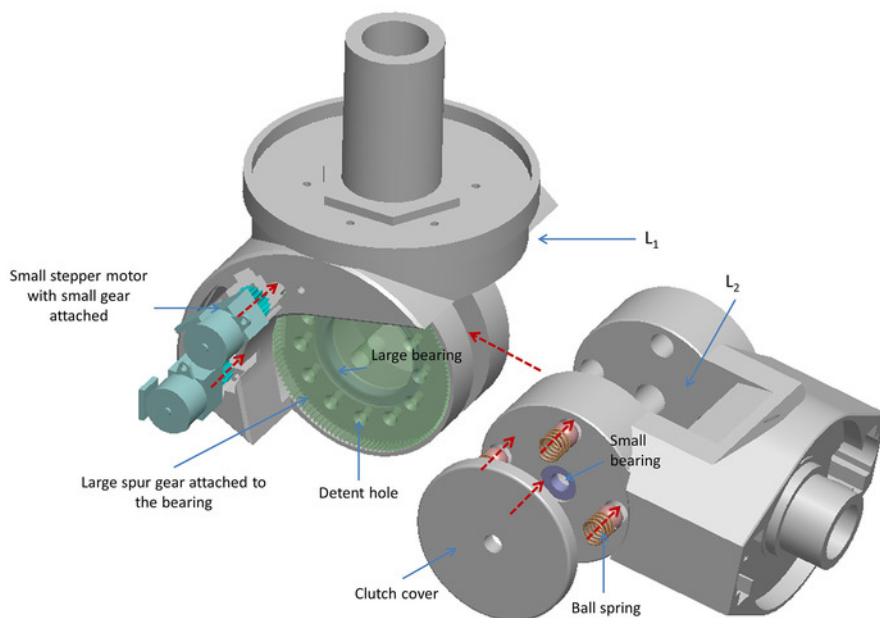


**Figure 4: Assembly instruction for J<sub>2</sub>.** The required links, motors, gears, ball-spring pairs, and bearings are shown, with some structures changed to transparent to illustrate the assembly. [Please click here to view a larger version of this figure.](#)



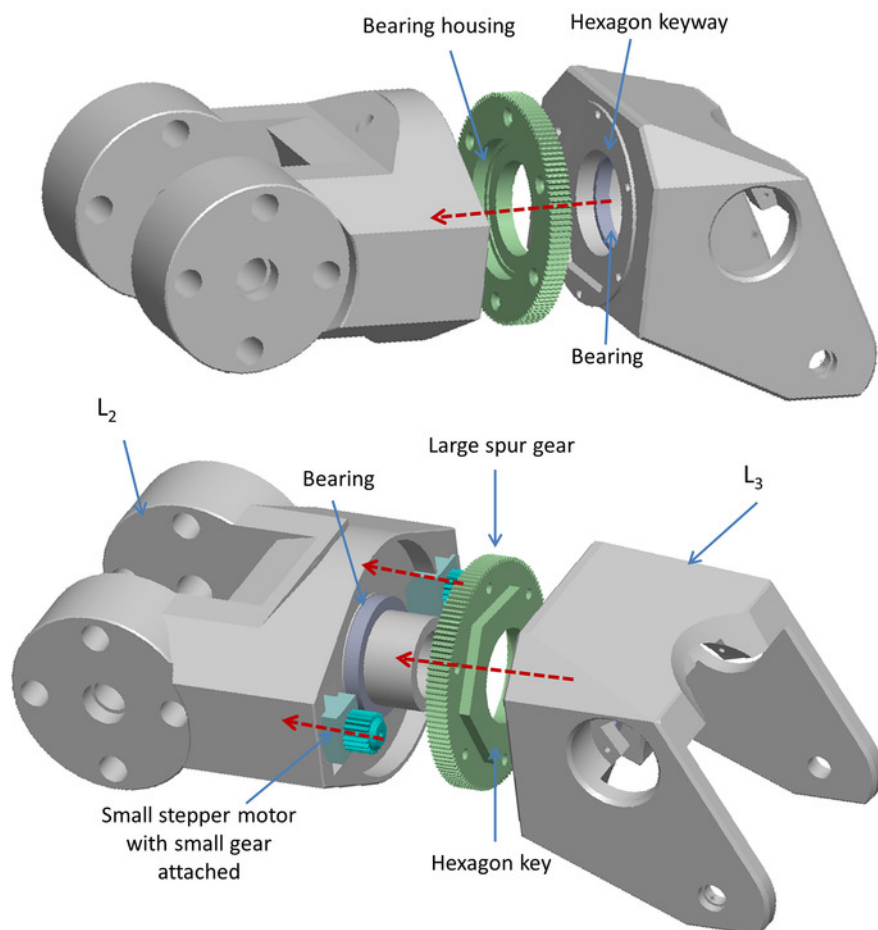


**Figure 5: Assembly instruction for J<sub>3</sub>.** The required links, motors, gears, and bearings are shown with two perspective views to illustrate the assembly. [Please click here to view a larger version of this figure.](#)

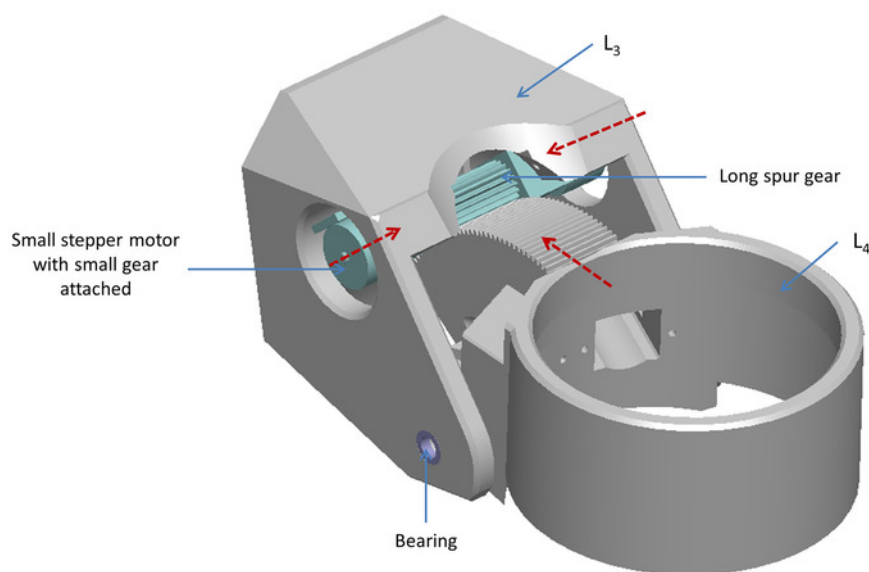


**Figure 6: Assembly instruction for J<sub>4</sub>.** The required links, motors, gears, and bearings are shown, with the assembled J<sub>4</sub> mechanism indicated. [Please click here to view a larger version of this figure.](#)

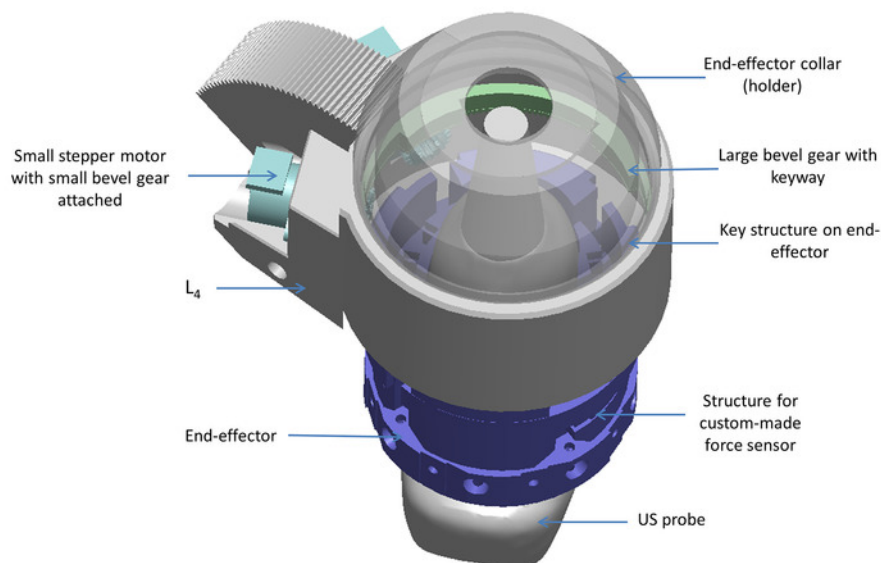


**Figure 7: Assembly instruction for  $J_5$ .** The required link and end-effector, motors, and gears are shown, with some structures changed to transparent to illustrate the assembly. [Please click here to view a larger version of this figure.](#)

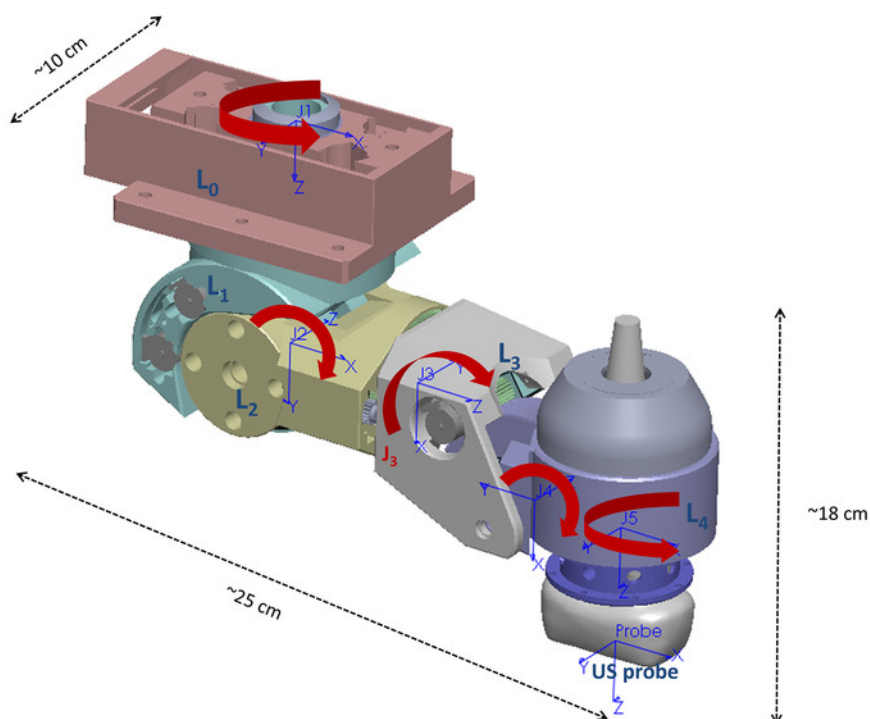


**Figure 8: Summary of the proposed 5-DOF robotic manipulator with the end-effector holding a US probe.** The coordinate definition of each joint and the overall size of the assembled manipulator are indicated. [Please click here to view a larger version of this figure.](#)

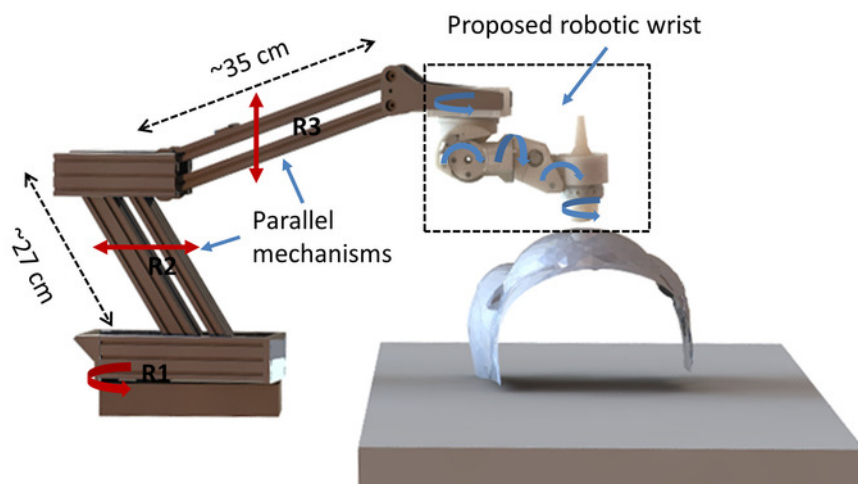


**Figure 9: CAD drawing of the example global positioning device.** This arm-based device is used to work with the proposed robotic manipulator for testing. The notations and the main dimensions are shown in the drawing. [Please click here to view a larger version of this figure.](#)

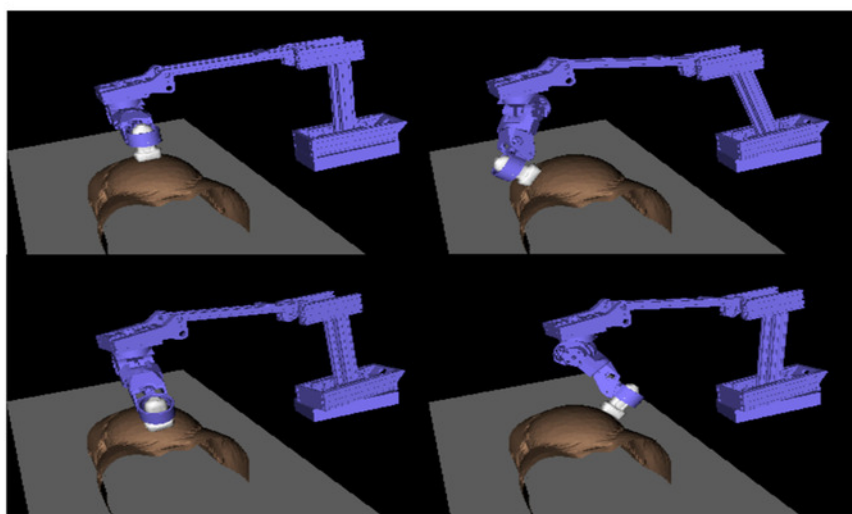


**Figure 10: Kinematic simulation of four different scanning postures around the phantom.** This demonstrates an adequate range of motion for a typical abdominal US scan. [Please click here to view a larger version of this figure.](#)

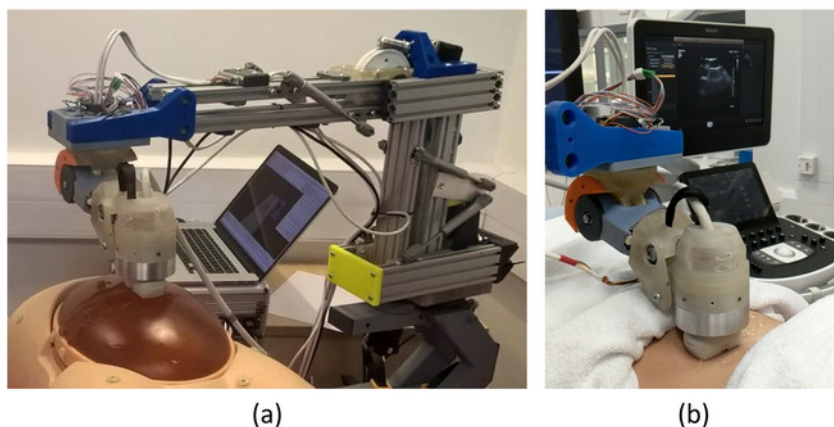


**Figure 11: Implemented US robot using the described protocol.** (a) The robotic manipulator with the example global positioning mechanism. (b) Clinical use of the proposed robotic manipulator on a patient's abdominal area. [Please click here to view a larger version of this figure.](#)



**Table of Materials: Technical details of the proposed robotic manipulator, including the Denavit-Hartenberg parameters and the joint specifications.** [Please click here to view a larger version of this figure.](#)

**Supplementary Files. 3D printable STL files.** [Please click here to download this file.](#)

## Discussion

Unlike many other industrial robots that have been translated into medical applications, the proposed robotic manipulator described in the protocol was specifically designed for US examinations according to clinical requirements for the range of motion, application of force, and safety management. The lightweight robotic manipulator itself has a wide range of movements sufficient for most extra-corporeal US scanning, without the need for large movements of the global positioning mechanism. As the closest mechanical structure to the patient, the proposed links are also specially shaped to be away from the patient. With most DOFs embedded into a compact manipulator, robotic US scanning using this device can be done in an intuitive way similar to human operation without the necessity of occupying a large space. Because of all these features, we expect that the system produced following the protocol could gain acceptance from clinicians and patients, which is being validated with the on-going volunteer study. With the proposed robotic manipulator, different conventional architectures for global positioning can be used based on the particular requirement, such as a gantry or ceiling mounting designs. An example global positioning device was used in this paper to enable the tests of the proposed robotic manipulator.

The current protocol suggests that all the links can be printed using ABS or PLA plastics or nylon, based on the availability of the local 3D-printing service, while using the nylon prints is preferred in general due to nylon's material strength. Importantly, as stated in the protocol, the additional components, especially the gears, should be printed with nylon or another strong material to ensure the reliability of the system. As new 3D-printing materials are introduced, the use of materials could be altered. The current protocol employs an end-effector specifically designed for a particular US probe, with the probe's 3D shape scanned by a CT imaging system to assist the design of the inner profile of the end-effector. When the manipulator is used with other US probes with different shapes, it is important to ensure that the inner profile of the end-effector is redesigned to tightly match with the outer profile of the US probe, in order to guarantee the safe holding of the probe. The 3D shape and profile of the probe could also be obtained from other types of 3D scanning. Additionally, it should be noted that some of the design details described in the protocol, such as exact shapes and dimensions, shaft sizes, mounting keyways, screws, and use of bearings, could be altered. For the same reason, some of the details are not provided when they are obviously based on common knowledge of mechanical design.

The current design has a passive mechanical clutch which can be adjusted and used to limit the maximum force applied to the patient. This is a safety feature that does not rely on any electrical systems or software logic, which guarantees the fundamental safety of using the robot for US examinations. The triggering point was set based on the range from previous measurements<sup>21</sup> of the vertical force applied by human operators to the patients during normal US scans, as well as similar results reported from the existing literature<sup>18</sup>, both of which suggest that the maximum vertical force usually does not exceed 20 N. This was treated as the prerequisite that the trigger force of the clutch should be more than 20 N with some given allowances. The amount of triggering force can be adjusted by changing the number of ball-spring pairs, the spring constant, the size of the detent holes, and the preloading of the springs<sup>22</sup>. A potential modification of the designed protocol for this is to change the number of cavities for holding the ball-spring pairs in  $L_2$ . In practice, when using the proposed system, the correct working of the clutch can be easily verified by manually rotating the clutch joint and having the clutch disengage and re-engage before any robotic US examination is performed. In the current protocol, the safety clutch is only applied to  $J_2$  as this joint is designed to align the probe with the surface of the abdomen and can be directly used to limit the vertical force exerted on the patient by the US probe. With a similar concept, a safety clutch can also be implemented for the  $J_1$  spur gear, which will ensure the safety of the  $J_1$  rotational movement of the following structures. This is not seen as an essential safety feature in the current protocol but could be a potential modification for a finalized version. The last three joints,  $J_3$ ,  $J_4$ , and  $J_5$ , are used for fine adjustments of the probe's orientation. Kinematically, they are not used to generate any excessive force and are not likely to collide with any obstacle. To minimize the size and weight of the proposed manipulator, a safety mechanical clutch is not suggested for these three joints in any modification of the protocol.

Following the protocol presented here to build the proposed manipulator for US examinations, the same reliability of the mechanical system, the same ranges of motion, similar weights of the whole manipulator, and a similar level of triggering force of the clutch are expected as are reported in this paper. However, the repeatability and accuracy of the movements, as well as the repeatability of the exact triggering force level of the mechanical clutch, would strongly depend on the 3D-printing and assembly accuracy compared to the CAD design. This cannot be guaranteed for the current prototype as a lab-based low-end 3D-printing service was used for manufacturing and the assembly was done manually for the purpose of preliminary prototyping. It is expected that an industrial level of manufacturing and assembly following the design protocol would result in good repeatability and high accuracy, although this is currently not our aim before the system is made into a final product for clinical trial. The testing of the performance would also require a separate protocol, which includes kinematic modeling, a robotic control method, motion tracking, and calibration methods, and is, thus, not included in the current paper. Similarly, the control precision and response of the proposed manipulator are determined by the motor control method, robot control algorithm, and communication between the electronics of the manipulator and the control interface. As these are beyond the aim of the current protocol of introducing the new mechanical design and can be implemented using many existing architectures, details are not provided in this paper.

## Disclosures

The authors have nothing to disclose.

## Acknowledgements

This work was supported by the Wellcome Trust IEH Award [102431] and by the Wellcome/EPSRC Centre for Medical Engineering [WT203148/Z/16/Z]. The authors acknowledge financial support from the Department of Health via the National Institute for Health Research (NIHR)

comprehensive Biomedical Research Centre award to Guy's & St Thomas' NHS Foundation Trust in partnership with King's College London and King's College Hospital NHS Foundation Trust.

## References

1. Priester, A. M., Natarajan, S., Culjat, M. O. Robotic ultrasound systems in medicine. *IEEE Transactions on Ultrasonics, Ferroelectrics, and Frequency Control*. **60** (3), 507-523 (2013).
2. Magnavita, N., Bevilacqua, L., Mirk, P., Fileni, A., Castellino, N. Work-related musculoskeletal complaints in sonologists. *Journal of Occupational and Environmental Medicine*. **41** (11), 981-988 (1999).
3. Jakes, C. Sonographers and Occupational Overuse Syndrome: Cause, Effect, and Solutions. *Journal of Diagnostic Medical Sonography*. **17** (6), 312-320 (2001).
4. Society of Diagnostic Medical Sonography. Industry Standards for the Prevention of Work-Related Musculoskeletal Disorders in Sonography: Consensus Conference on Work-Related Musculoskeletal Disorders in Sonography. *Journal of Diagnostic Medical Sonography*. **27** (1), 14-18 (2011).
5. LaGrone, L. N., Sadasivam, V., Kushner, A. L., Groen, R. S. A review of training opportunities for ultrasonography in low and middle income countries. *Tropical Medicine & International Health*. **17** (7), 808-819 (2012).
6. Shah, S. *et al.* Perceived barriers in the use of ultrasound in developing countries. *Critical Ultrasound Journal*. **7** (1), 28 (2015).
7. Swerdlow, D. R., Cleary, K., Wilson, E., Azizi-Koutenaei, B., Monfaredi, R. Robotic Arm-Assisted Sonography: Review of Technical Developments and Potential Clinical Applications. *American Journal of Roentgenology*. **208** (4), 733-738 (2017).
8. Nouaille, L., Laribi, M., Nelson, C., Zeghloul, S., Poisson, G. Review of Kinematics for Minimally Invasive Surgery and Tele-Echography Robots. *Journal of Medical Devices*. **11** (4), 040802 (2017).
9. Georgescu, M., Saccomandi, A., Baudron, B., Arbeille, P. L. Remote sonography in routine clinical practice between two isolated medical centers and the university hospital using a robotic arm: a 1-year study. *Telemedicine and e-Health*. **22** (4), 276-281 (2016).
10. Arbeille, P. *et al.* Use of a robotic arm to perform remote abdominal telesonography. *American Journal of Roentgenology*. **188** (4), W317-W322 (2007).
11. Arbeille, P. *et al.* Fetal tele#echography using a robotic arm and a satellite link. *Ultrasound in Obstetrics & Gynecology*. **26** (3), 221-226 (2005).
12. Vieyres, P. *et al.* A tele-operated robotic system for mobile tele-echography: The OTELO project. In *M-Health: Emerging Mobile Health Systems*. Edited by Istepanian, R. H., Laxminarayan, S., Pattichis, C. S., 461-473, Springer. Boston, MA (2006).
13. Abolmaesumi, P., Salcudean, S. E., Zhu, W.H., Sirouspour, M. R., DiMaio, S. P. Image-guided control of a robot for medical ultrasound. *IEEE Transactions on Robotics and Automation*. **18** (1), 11-23 (2002).
14. Abolmaesumi, P., Salcudean, S., Zhu, W. Visual servoing for robot-assisted diagnostic ultrasound. *Engineering in Medicine and Biology Society, Proceedings of the 22nd Annual International Conference of the IEEE*. Chicago, IL July 23-28 (2000).
15. Menikou, G., Yiallouras, C., Yiannakou, M., Damianou, C. MRI#guided focused ultrasound robotic system for the treatment of bone cancer. *The International Journal of Medical Robotics and Computer Assisted Surgery*. **13** (1), e1753 (2017).
16. Yiallouras, C. *et al.* Three-axis MR-conditional robot for high-intensity focused ultrasound for treating prostate diseases transrectally. *Journal of Therapeutic Ultrasound*. **3** (1), 2 (2015).
17. AdEchoTech. *MELODY, a remote, robotic ultrasound solution*. <http://www.adechotech.com/products/> (2018).
18. Essomba, T. *et al.* A specific performances comparative study of two spherical robots for tele-echography application. *Proceedings of the Institution of Mechanical Engineers, Part C: Journal of Mechanical Engineering Science*. **228** (18), 3419-3429 (2014).
19. Bassit, L. A. *Structure mécanique à modules sphériques optimisées pour un robot médical de télé-échographie mobile*. PhD thesis. Université d'Orléans, France (2005).
20. Noh, Y. *et al.* Multi-Axis force/torque sensor based on Simply-Supported beam and optoelectronics. *Sensors*. **16** (11), 1936 (2016).
21. Noh, Y. *et al.* An ergonomic handheld ultrasound probe providing contact forces and pose information. *Engineering in Medicine and Biology Society, Proceedings of the 37th Annual International Conference of the IEEE*. Milan, Italy August 25-29 (2015).
22. Maplesoft. *Translational Detent – MapleSim Help*. <https://www.maplesoft.com/support/help/MapleSim/view.aspx?path=DrivelineComponentLibrary/translationalDetent> (2018).